Int. J. Nanosci. Nanotechnol., Vol. 19, No. 4, Dec. 2023, pp. 295-306
DOI: 10.22034/ijnn.2023.2011036.2424

An Orderly-Arranged Attapulgite/PIM-1 Mixed Matrix Membranes for Gas Separation

Hongyong Zhao[1,2], Fengqiu Guo[1,2], Xiaoli Ding[1,3,*], Xiaoyao Tan[1,2] and Yuzhong Zhang[1,3]

[1]State Key Laboratory of Separation Membranes and Membrane Processes/National Center for International Joint Research on Separation Membranes, Tiangong University, Tianjin 300387, China
[2]School of Chemical Engineering and Technology, Tiangong University, Tianjin 300387, China
[3]Institute of Separation Material and Process Control, School of Material Science and Engineering, Tiangong University, Tianjin 300387, China

(*) Corresponding author: dingxiaoli@tiangong.edu.cn
(Received: 07 September 2023 and Accepted: 16 November 2023)

Abstract

Developing mixed matrix membranes (MMMs) is a way to fabricate high permeation-performance membranes. The arrangement of the fillers, especially the specific-shaped ones, in the membranes has a non-negotiable influence on the gas-transport performance. With the assistance of a magnetic field, the Fe_3O_4 decorated attapulgite (ATP) is orderly arranged into the polymer of intrinsic microporosity (PIM-1) to form ATP/PIM-1 MMMs. Moreover, Fe_3O_4 decorated ATPs were coated with polydimethylsiloxane to avoid the polymeric matrix filling the cavity of ATPs. Chemical compositions of modified ATPs were determined by Fourier transform infrared spectroscopy. Morphologies of modified ATPs were observed via transmission electron microscopy and wide-angle X-ray diffraction. Morphologies of ATP/PIM-1 MMMs investigated by field-emission scanning electron microscopy. The effects of the vertically-arranged, parallelly-arranged, and disorderly-arranged ATPs on gas permeation-separation performances of ATP/PIM-1 MMMs were also reported. The parallelly-arranged ATP/PIM-1 MMMs display the best gas permeability compared with vertically-arranged and disorderly-arranged ATP/PIM-1 MMMs. And introducing the parallelly-arranged ATP brings about higher gas permeability and selectivity. Compared with the original PIM-1 membrane, the parallelly-arranged ATP/PIM-1 MMM with 5 wt.% ATP loading shows CO_2 permeability of ~4018 Barrer coupled with CO_2/N_2 selectivity of ~19, and O_2 permeability of ~672 Barrer coupled with O_2/N_2 selectivity of ~3. The CO_2 permeability and O_2 permeability increases to ~2.7 times.

Keywords: *Air separation, CO_2 separation mixed matrix membrane, Attapulgite, Ordered arrangement.*

1. INRODUCTION

Gases are important resources, which have been widely used in many production-machining fields [1-2]. As one of the important industrial processes, gas separation can be performed by adsorption and absorption, cryogenic treatment, membrane technology, etc. [3-5] Among them, gas separation membrane technology has been a central industrial unit [6]. Polymeric membranes with high gas permeability and selectivity are always desired. But a trade-off between gas permeability and selectivity has been recognized [7-9]. Developing mixed matrix membranes (MMMs) is a way to improve gas permeation-separation performance and exceed the trade-off. Much academic research focused on introducing porous fillers and nonporous fillers to membranes [5, 10-21]. The nonporous fillers, containing nano-size inorganic particles and organic particles, are usually nano-sized and can change the packing of the chain segment to improve

the gas permeation-separation performance; and the porous fillers, such as zeolites, carbon tube, and carbon molecular sieves, exhibit excellent cavities and channels to supply the good gas transport or size-sieving ability.

Recently, environmentally friendly materials have gotten more and more attention, and many researchers also focus on membranes based on natural materials [22-23]. Attapulgite (ATP) is a magnesium-aluminosilicate clay mineral with many chain-layered units, which is composed of 2:1 tetrahedral sheets and octahedral sheets [24, 25]. These units are connected via tetrahedral sheets to form an orderly layered accumulation body. A tunnel-like cavity forms between these units, and its cross section is the size of 3.7 × 6.3 Å rectangular microspores shown in Fig.1, which are favorable to gas transport and separation. Therefore, it has the potential to enhance the gas permeation-separation performance by incorporating ATP with the polymeric membranes. The ATP/Pebax1657 MMMs prepared in Pan's group [26], and exhibited a better CO_2 permeability and CO_2/N_2 selectivity compared with the original Pebax membrane. They subsequently deposited an ultrathin ATP/Pebax MMMs selective layer (~700 nm) on a porous polyacrylonitrile supporting membrane [27]. The composite membranes showed improved CO_2 permeance and CO_2/N_2 and CO_2/CH_4 selectivities. Ahmad et al. investigated the effect of different solvents (NMP, DMF) on the gas permeation-separation performance of the ATP/Pebax-1657 MMMs [28]. And it showed that the ATP/Pebax-1657 MMMs prepared with NMP displayed better solubility. At 3 wt.% of ATP loading, the MMMs prepared with NMP solvent showed higher CO_2 permeability and CO_2/ N_2 selectivity compared with those prepared with DMF solvent. Wang et al [29] investigated the use of ATP as a filler added to CMS membranes for performance enhancement, and the addition of ATP not only improved the thermal stability of CMS membranes, but also improved the average pore size and gas separation performance of CMS membranes.

On the one hand, for inorganic fillers, the undesirable organic-inorganic interface defects [20], which usually cause a negative influence on gas permeation-separation performance, should be seriously solved in time. On the other hand, for fillers with narrow cavities or pores, different arrangements of fillers can lead to different effects. As shown in Fig.1, if the direction of narrow pores is parallel to the gas-permeation direction, it will provide the best promotion to gas permeation-separation performance; if the direction is perpendicular to the gas-permeation direction, it will bring negative effects. Because in this direction of the narrow channel, the pressures and concentrations at both ends of the narrow pore are very close, the driving force of pressure and concentration is barely available, and the gas slowly permeates through the channel, and even some gas residues in the channel.

In this study, to the shortcomings of inorganic ATP fillers, firstly, we adsorbed Fe_3O_4 particles on the surface of the ATP fillers. And then, the ATP fillers were coated with high-gas-permeability polydimethylsiloxane (PDMS). The PDMS layer can provide an organic interface to eliminate organic-inorganic interface defects. And PDMS exhibits high gas permeability and can ensure gas permeate freely in ATP channels. Moreover, the PDMS layer can prevent the polymeric matrix from entering the ATP channels in the process of MMMs preparation, which will cause the ATP channels ineffective. Secondly, according to the principle that magnetic particles always arrange in the direction of the magnetic induction line under a strong magnetic field. With the assistance of a magnetic field and the adsorbed Fe_3O_4 particles on the surface of the ATP, the ATP was orderly arranged into the polymer of intrinsic

microporosity-1 (PIM-1) matrix to form the ATP/PIM-1 MMMs. The gas permeation properties in ATP/PIM-1 MMMs were tested. The influences of the vertically-arranged ATP, the parallelly-arranged ATP, and the disorderly-arranged ATP on gas permeation properties were investigated.

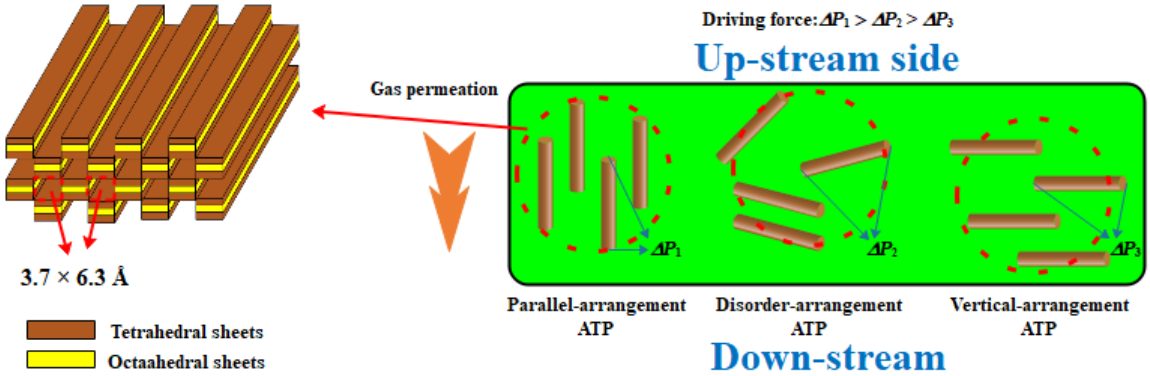

Figure 1. *Diagram of ATP structure and arrangement in MMMs.*

2. EXPERIMENTAL

2.1. Materials

PIM-1 was prepared according to the process reported in our previous work [30]. The ATP obtained from Guangzhou Tuoyi Trading Co., iso-octane supplied by Tianjin Kemiou Chemical Reagent Co., Ltd, PDMS (RTV615) produced by Beijing Zhongke Lang Yi Technology Co., $FeCl_2 \cdot 4H_2O$ provided by Tianjin Guangfu Fine Chemical Research Institute, $FeCl_3 \cdot 6H_2O$, NaOH and ethanol supplied by Tianjin Wind Ship Chemical Reagent Technology Co., N_2, O_2, and CO_2 provided by Tianjin Huanyu Gas Development Center and used as received. The experimental procedures used were all deionized water.

2.2. Pre-Treatment of ATP

2.2.1. Prepare the Fe_3O_4-Decorated ATP

Dispersed original ATP in deionized water and washed them several times to remove some soluble impurities. Dissolved the iron salt in deionized water (molar ratio of Fe^{2+}:Fe^{3+}=1:2). Added the ATP to the ionic solution under N_2 protection with rapid stirring for 30 min at 70 °C under reflux, then added 1mol·L^{-1} NaOH solution drop by drop. As the pH increased, the color of the solution changed from dark brown to dark orange due to generating ferric hydroxide, then to dark green, and finally to black caused by Fe_3O_4 particles, continued stirring for 3 h, cooling down and standing for 24 h. Filtered the solution, washed with ethanol and water alternately to neutral, and dried at room temperature to obtain the Fe_3O_4- decorated ATP.

2.2.2. Fe_3O_4-decorated ATP Coated by PDMS

Soaked and wetted a certain amount of Fe_3O_4-decorated ATP with deionized water, which can prevent the PMDS solution from entering the ATP channel. Left the surface of the ATP to dry, washed with 2 wt.% of PDMS solution several times, dried for 24 h at 25 °C, and then dried at 100 °C for 48 h in a vacuum oven to obtain the PDMS-coated ATP.

2.3. Fabrication of ATP/PIM-1 MMMs

The pre-treated ATP with different mass ratios was added to the PIM-1 solution (2 wt.% in chloroform). The mixture was ultrasonicated for 0.5 h and stirred for 2 h. Then the mixture solution was cast on a glass board. Meanwhile, a magnetic field with vertical or parallel directions was applied to the membrane in the process of evaporation at 25°C for 2 d as illustrated in Fig.2. The magnetic field was provided by a magnetic stand (8T, Sanliang, Japan).

The nascent MMMs dried in a vacuum oven at 80°C for 24 h. The thickness of the MMMs is about ~ 50 μm. In addition, following the above-mentioned steps, the ATP/PIM MMMs were also fabricated without the magnetic field for comparison. The overall process of fabricating the ATP/PIM-1 MMMs is shown in Fig. 2.

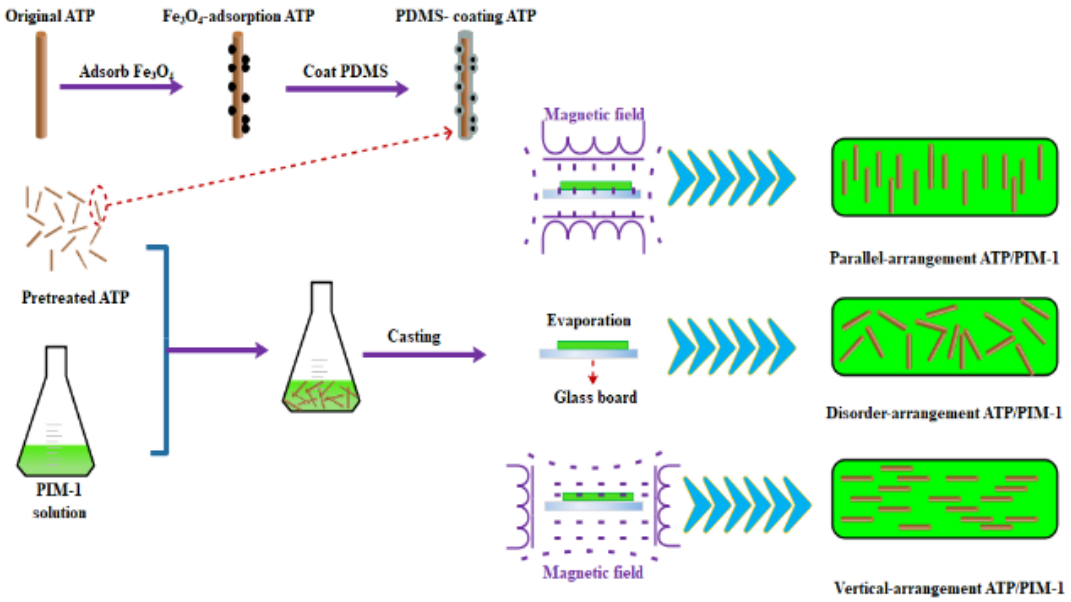

Figure 2. *Scheme of synthesizing the ATP/PIM-1 MMMs.*

2.4. Fourier Transform Infrared (FTIR) Spectroscopy

FTIR was used to investigate the chemical composition of original ATP, Fe_3O_4-decorated ATP, and PDMS-coated ATP. The spectrum was accumulated from 400 to 4000 cm^{-1} at a resolution of 4 cm^{-1}.

2.5 Morphology Study of ATP Particles

The morphologies of original ATP, Fe_3O_4-decorated ATP, and PDMS-coated ATP were characterized by transmission electron microscope (TEM). The samples were prepared by spreading the dilute suspension of the ATP particles on a carbon support membrane.

2.6. Wide Angle X-Ray Diffraction (WAXD)

WAXD patterns of ATP particles and ATP/PIM-1 MMMs were studied by using a Scintag theta-theta diffractometer. And samples were measured with a 2θ scan from 2 ° to 40 ° with a 0.05 ° step. The *d*-spacing, corresponding to the position of diffraction maximum, calculated via Bragg's Law: $d\text{-spacing} = \lambda/2\sin\theta$, where λ is 1.54 Å of wavelength, and θ is the angle of the reflection peak (°).

2.7. Membrane Morphology

The cross-sections and surface morphology of ATP/PIM-1 MMMs were characterized using field-emission scanning electron microscopy (FESEM). The samples were sputter-coated with gold to increase their electrical conductivity.

2.8. Permeation Measurement

Gas permeability for O_2, N_2, and CO_2 of the ATP/PIM-1 MMMs tested by using a constant-volume/variable-pressure apparatus (2 atm and 35°C). Permeability coefficient (P) reported in a unit of cm^3 (STP) cm cm^{-2} s^{-1} $cmHg^{-1}$ and commonly expressed in a unit of Barrer (1 Barrer = 10^{-10} cm^3 (STP) cm cm^{-2} s^{-1} $cmHg^{-1}$). The ideal selectivity is defined as follows: $\alpha_{A/B} = P_i/P_j$, where the subscripts "i" and "j" are gas i and j, respectively. Diffusion coefficient (D, cm^2 s^{-1}) obtained by the time-lag method as $D = L^2/6\theta^*$, where θ^*

(s) is the diffusivity time-lag and L (cm) is the thickness of the symmetric membrane. The ratio of D_i over D_j is termed diffusion selectivity (α_D). Solubility coefficient (S, $cm^3(STP)\cdot cm^{-3}\cdot cmHg^{-1}$) is evaluated as follows: $S = P/D$. The ratio of S_i over S_j is termed solubility selectivity (α_S).

3. RESULTS AND DISCUSSION

3.1. Characterization of ATP Particles

As shown in Fig.3, ATP shows peaks at ~3600 cm^{-1}, attributed by ν(Mg-OH) and ν(Al-OH), and the absorption peaks at ~1115 cm^{-1} and ~525 cm^{-1} are due to the stretching vibration of the Si-O bond in ATP [31]. Fe_3O_4-decorated ATP and PDMS-coated ATP show the characteristic absorption peak of the Fe-O bond at ~630-650 cm^{-1}. It indicates Fe_3O_4 particles adsorbed on the surface of ATP. A characteristic peak of Si-CH_3, meanwhile, can be found in the spectra of the PDMS-coated ATP. It is because Fe_3O_4-decorated ATP is coated with the PDMS. The weak intensity of this peak also indirectly indicates PDMS coating layer is thin.

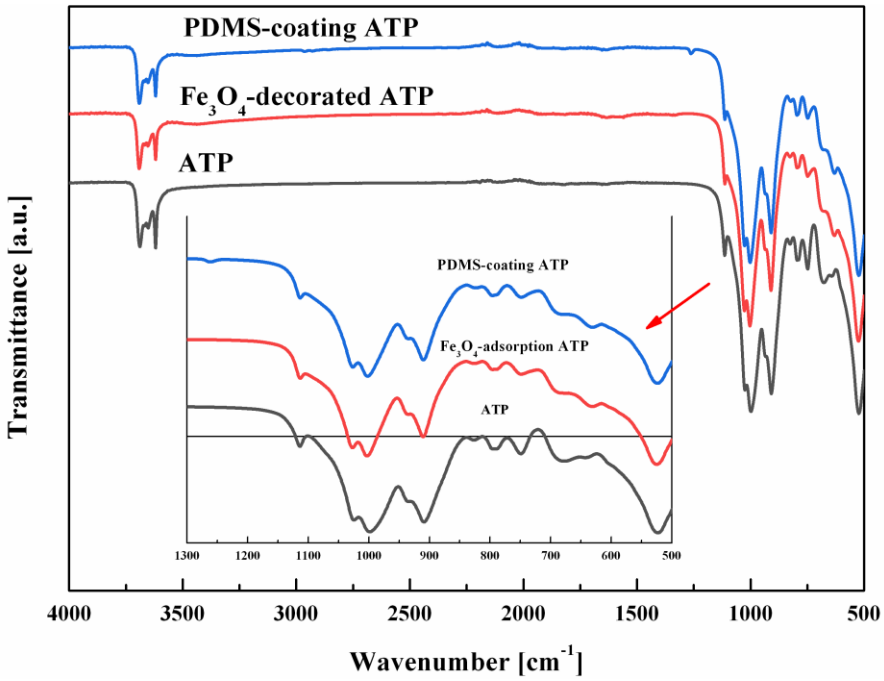

Figure 3. *Comparison of FTIR spectra of original ATP, Fe_3O_4-decorated ATP, and PDMS-coated ATP.*

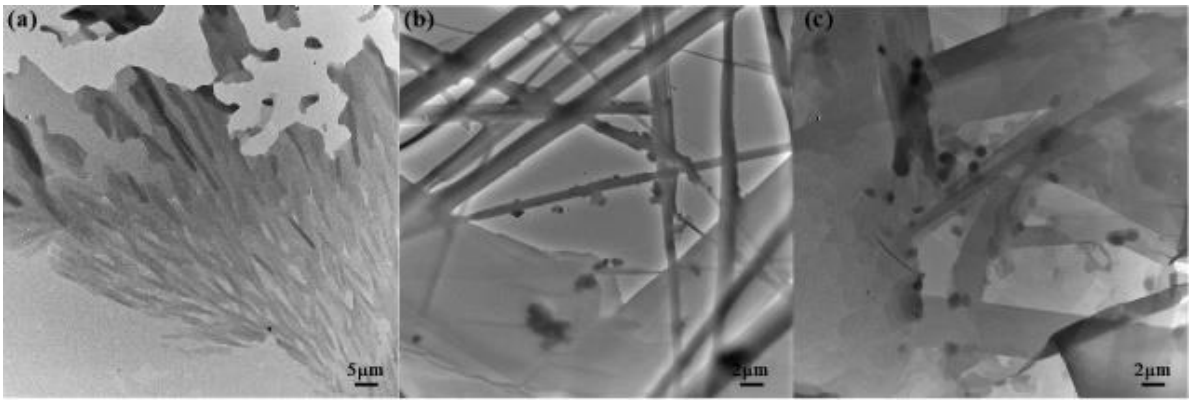

Figure 4. *TEM images of the ATP particles: (a) original ATP and (b) Fe_3O_4-decorated ATP, and (c) PDMS-coated ATP.*

TEM analysis was processed to investigate the structure of the ATP particles. As seen in Fig. 4(a), the ATP particles show inner-hollow narrow cavities and possess a diameter of about ~1.5-2 μm, which contains ~1 × 10^6 to 1 ×10^7 narrow channels (3.7 × 6.3 Å). Compared with the original ATP, as shown in Fig.4(b), Fe_3O_4 particles are attached to the surface of the ATP and do not enter the narrow channels, which avoids the influence of gas permeating through the channel. Since the size of Fe_3O_4 particles is much larger than the size of the channels. Fig.4(c) shows that the PDMS-coated ATP has a smoother surface than Fe_3O_4-decorated ATP, and still has a good inner-hollow structure. It again indicates that the Fe_3O_4-decorated ATP was coated by the PDMS, and the PDMS coating solution did not enter the channels. Moreover, the Fe_3O_4 particles have an additional fixing effect by the PDMS coating layer.

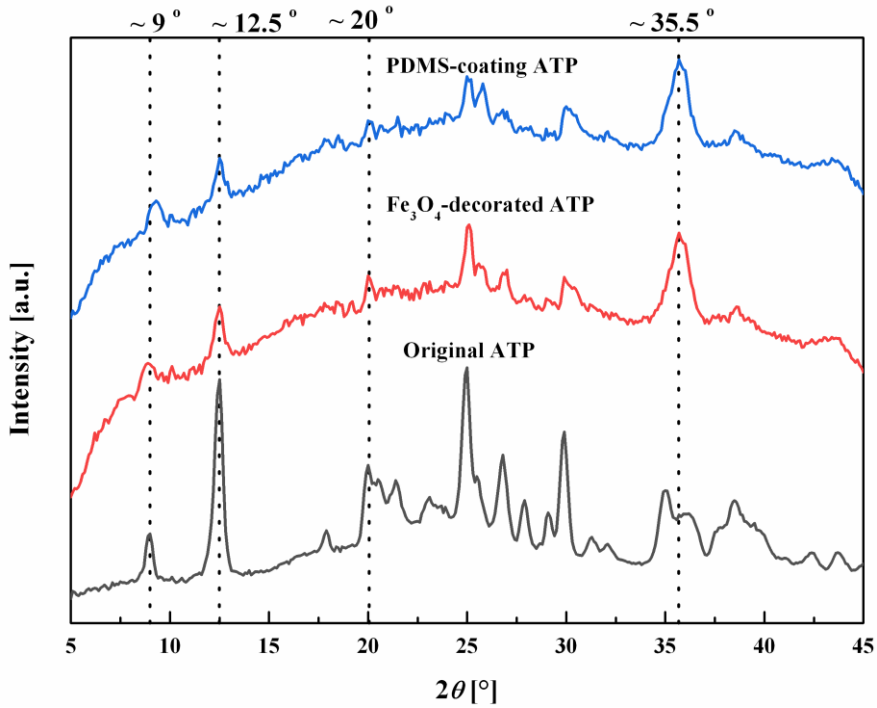

Figure 5. *XRD patterns of original ATP, Fe_3O_4-decorated ATP, and PDMS-coated ATP.*

As shown in Fig.5, the original ATP displays a crystalline clay. The peak of ~9 °, corresponding to an interlayer distance of ~10.4 Å, is attributed to the basic framework of the ATP [32]. The peaks of ~12.5 ° and ~20 ° represent the hydrated oxides with Mg^{2+} between layers and the Si-O-Si crystalline layers. Moreover, the peak of ~25 ° is attributed to the quartz impurities, which affect and weaken the intensity of the major peaks (at ~9 °, ~12.5 °, and ~20 °). Compared with the original ATP, both Fe_3O_4-decorated ATPs and PDMS-coated ATPs show a different peak at ~35.5 °, one of the characteristic peaks of Fe_3O_4 particles. Fe_3O_4-decorated ATP and PDMS-coated ATP also show major peaks of ~9 °, ~12.5 °, and ~20 ° corresponding to the ATP framework. It indicates that the procedure of adsorbing Fe_3O_4 particles and coating PDMS did not destroy the main framework of ATP. Therefore, the narrow channels of ATP should also be better retained. However, the intensity of the major peaks (at ~9 °, ~12.5 °, and ~20 °) of Fe_3O_4-decorated ATPs, and PDMS-coated ATPs is lower than that of the original ATP. It is probably because Fe_3O_4 particles and the PDMS layer resemble impurities or pollutants on the surface of ATP and will also affect the peak intensity of ATP.

3.2. Characterization of the ATP/PIM-1 MMMs

Fig. 6 shows the SEM surface and cross-section morphology of ATP/PIM-1 MMMs. As to observe orderly-arranged ATP more clearly, the ATP/PIM-1 MMMs with high loading were selected. As seen from the surface morphology in Fig. 6(a) and 6(b), parallelly-arranged ATP mostly shows only a point on the surface of membranes; on the contrary vertically-arranged ATP show a tightly-arranged line-by-line on the surface of the membrane. Fig.6(c) and 6(d) show that the ATP particles arrange along the direction of the magnetic field line. However, some large ATP aggregates can also be found. It is probably a result of the high loading of ATP and the attraction between Fe_3O_4 particles under the strong magnetic field.

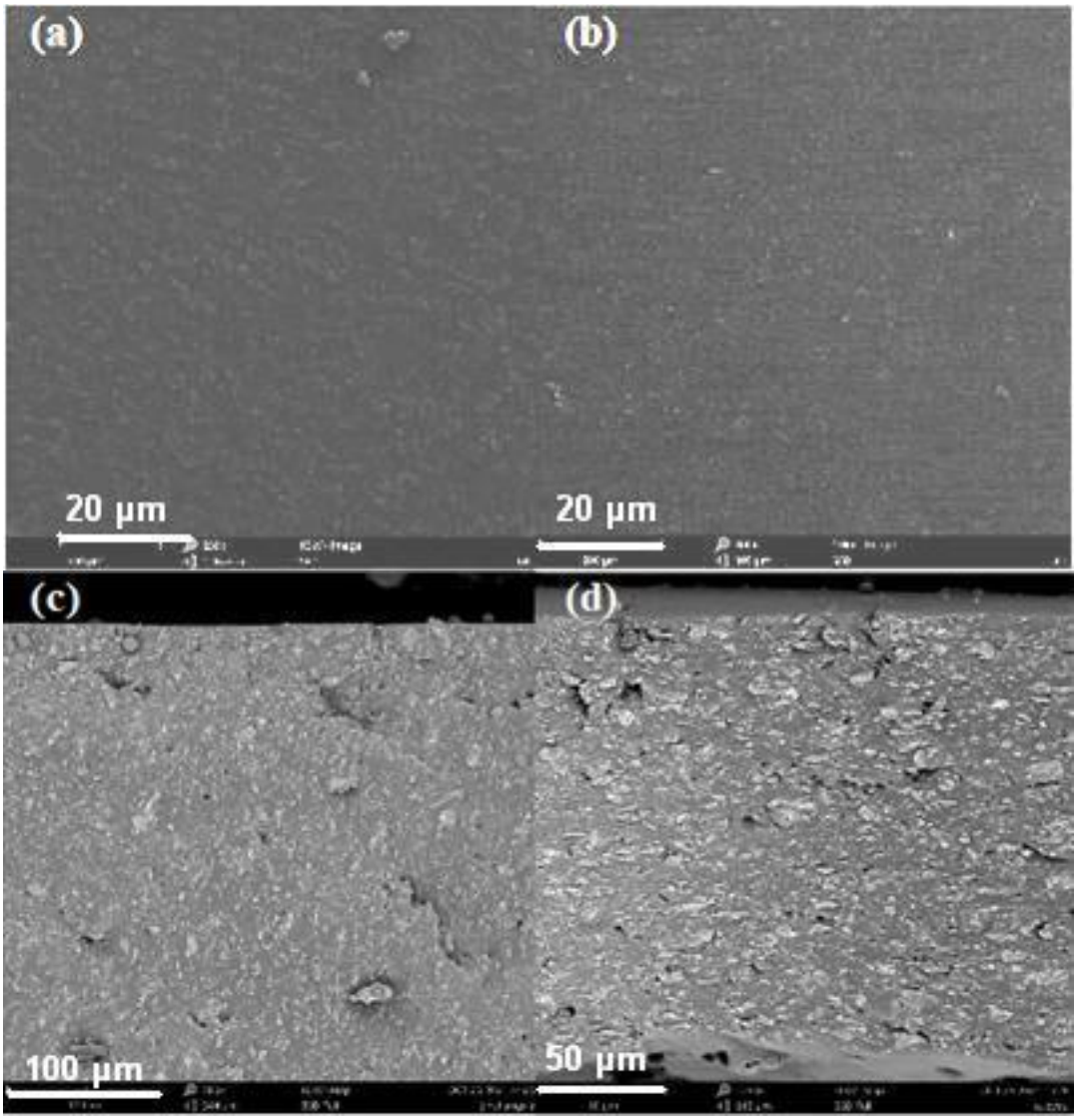

Figure 6. *SEM images of the ATP/PIM-1 MMMs (30 wt.% ATP loading): (a) surface morphology of parallelly-arranged ATP/PIM-1 MMMs, and (b) surface morphology of verticall-arranged ATP/PIM-1 MMMs, (c) cross-section morphology of parallelly-arranged ATP/PIM-1 MMMs, and (d) cross-section morphology of vertically-arranged ATP/PIM-1 MMMs.*

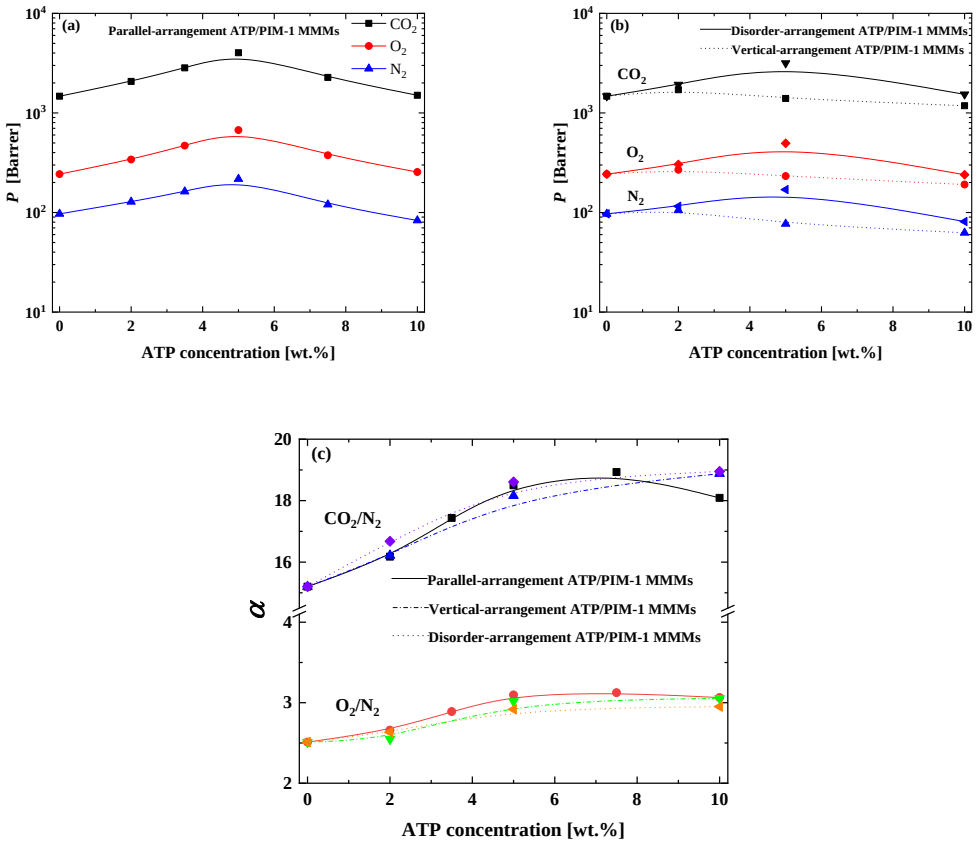

Figure 7. *Gas permeability and selectivity of the ATP/PIM-1 MMMs. ((a). gas permeability of Parallel-arrangement ATP/PIM-1 MMMs; (b) gas permeabilities of vertical- arrangement ATP/PIM-1 MMMs and disorder- arrangement ATP/PIM-1 MMMs; (c) gas selectivity of the ATP/PIM-1 MMMs).*

The permeability coefficient and selectivity of ATP/PIM-1 MMMs are illustrated in Fig.7. As illustrated in Fig.7(a), gas permeability coefficients firstly increase and then decrease as increasing the loading of the ATP in the parallelly-arranged ATP/PIM-1 MMMs. CO_2 and O_2 permeability increase to ~ 2.7 times. It discloses that the ATP provides a good gas transfer channel as expected, but as increasing the ATP content, more ATP aggregates are probably formed and result in a decrease in gas permeability. Compared with the parallelly-arranged ATP/PIM-1 MMMs, the disorderly-arranged ATP/PIM-1 MMMs also display a first increase and then a decrease in gas permeability with increasing ATP loading as shown in Fig.7(b). However, the increase is not more than the parallelly-arranged ATP/PIM-1 MMMs. It indicates that the parallelly-arranged ATP is more favorable to gas permeation than the disorderly-arranged ATP. The vertically-arranged ATP/PIM-1 MMMs show a different trend. Gas permeability slightly increases only at 2% ATP loading, and gas permeability significantly decreases with increasing ATP loading. As expected, vertically-arranged ATP is averse to gas transport and even hinders gas permeation. It also shows that CO_2/N_2 and O_2/N_2 selectivity first increase, then stabilize as the ATP loading increases. It discloses that narrow channels (3.7 × 6.3 Å) of ATP exhibit separation capacity of CO_2/N_2 and O_2/N_2 gas pairs, though the 3.7 Å is larger than gas-molecular diameters of CO_2, O_2, and N_2. Notably, the vertically-arranged ATP also displays a high selective ability as unexpected. It indicates that the channels of vertically-arranged ATP are

still available for gas transport but probably provide slow permeation to gases because of low-pressure driving forces as described in Fig.1. Therefore, the gas permeating through the narrow channels of ATP can still be separated, finally leads to an increase in gas selectivity.

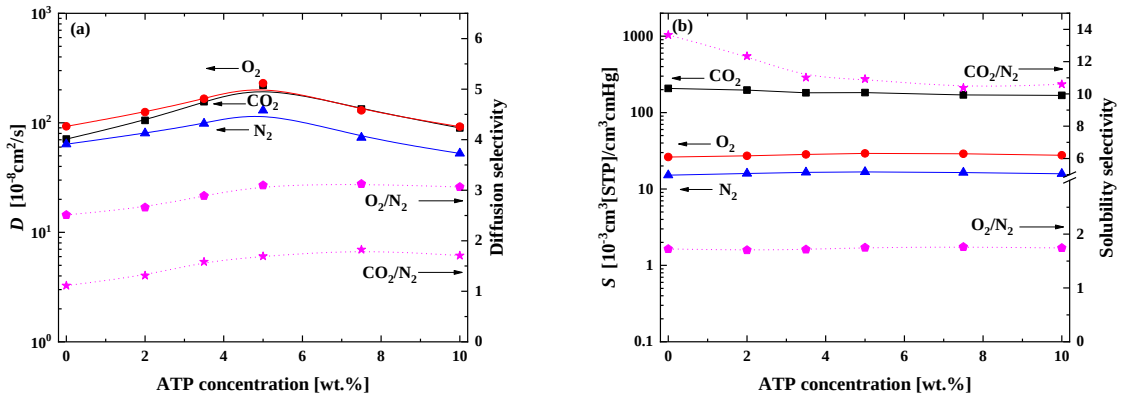

Figure 8. *Gas diffusivity and solubility of parallelly-arranged ATP/PIM-1 MMMs. ((a). Diffusion and diffusion selectivity of Parallel-arrangement ATP/PIM-1 MMMs; (b) Solubility and solubility selectivity of Parallel-arrangement ATP/PIM-1 MMMs).*

To further investigate the effect of ATP, gas solubility and diffusivity of parallelly-arranged ATP/PIM-1 MMMs have been estimated. As shown in Fig.8a, the original PIM-1 membrane displays higher O_2 diffusivity than CO_2 diffusivity. It leads to higher O_2/N_2 diffusivity selectivity than CO_2/N_2 diffusivity selectivity. It is a result of the order of gas diameter ($N_2 > CO_2 > O_2$), according to the effective diameter, the Dal-Cin correlation diameter, and the Robeson diffusion correlation diameter [9]. This result is consistent with other literature results [30, 33]. As seen from Fig 8(a) and 8(b), the gas diffusivity increases firstly and then decreases, the gas solubility of O_2 and N_2 almost keeps constant, and only the CO_2 solubility slightly decreases, as increasing the loading of the ATP in the parallelly-arranged ATP/PIM-1 MMMs. It indicates that the increase in gas permeability attributes mainly to an increase in gas diffusivity. Although the ATP exhibits a porous structure, its gas-sorption capacity is still much weaker than that of the PIM-1 matrix. Moreover, CO_2 has a high critical temperature and is sensitive to the change of gas-sorption sites. Therefore, as increasing ATP loading, the CO_2 solubility decreases slightly. It also shows that the CO_2/N_2 and O_2/N_2 diffusion selectivity increase, the O_2/N_2 solubility selectivity keeps constant, and the CO_2/N_2 solubility selectivity decreases with increasing the ATP loading. It discloses that the increase in diffusion selectivity contributes to the increase in gas selectivity. In summary, the increases in gas permeability and selectivity attribute mainly to the increases in gas diffusivity and diffusion selectivity. The narrow channels of ATP facilitate gas diffusion and provide a high sieving-size ability. However, the introduction of ATP also leads to a decrease in gas-sorption sites and causes a decrease in gas solubility. The gas permeation and separation properties of MMMs incorporated with ATP in this study were compared with those in the reported literature as illustrated in Table 1. ATPs can significantly increase the permeation performance, while the positive effect on selectivity was not as pronounced as on permeation.

Table 1. *Gas permeation and separation property comparison between some membranes reported in literatures and this study.*

Matrix	Filler	Permeability [Barrer]		Selectivity			Test condition	Ref.
		CO_2	O_2	CO_2/N_2	CO_2/CH_4	O_2/N_2		
Pebax®1657	ATP	120.2 (67%)	-	69.3 (61%)	-	-	3 atm, 40 °C	[28]
Pebax®1657	ATP	77.0 (38%)	-	52.0 (30%)	-	-	4 bar, 35 °C	[26]
Pebax®1657[a]	ATP	72.0 (12%)	-	50.0 (27%)	29.0 (9%)	-	4 bar, 35 °C	[27]
Cellulose	ATP	65.5 (680%)	-	43.7 (487%)	-	-	0.2 MPa, 25°C	[34]
Polyimide based carbon	ATP	636.2 (174%)	384.5 (93%)	8.3(-20%)	-	5.0 (-44%)	0.05 MPa, 30 °C	[29]
Polyimide[b]	KH-550 modified ATP	4.5 (152%)	0.8 (140%)	35.1 (-3%)	46.4 (1%)	6.5 (-8%)	4 atm, 308 K	[35]
PIM-1	Fe_3O_4-decorated ATP	4018.0 (273%)	672 (277%)	18.9 (21%)	-	3.1 (23%)	2 atm, 35 °C	This study

[a] Pyromellitic dianhydride/4,4-diaminodiphenyl ether
[b] composite membrane
(+ve): increment from the neat polymer membrane; (-ve): decrement from the neat polymer membrane; -: not available.

4. CONCLUSION

A series of orderly-arranged ATP/PIM-1 MMMs were prepared. The chemical composition, morphology and structure of the pre-treated ATP were confirmed via the TEM, WAXD, and FTIR. The morphology of the ATP/PIM-1 MMMs also investigated by SEM. Gas transport properties of ATP/PIM-1 MMMs performed. Different arrangements of ATP display a significant influence on gas permeability. Compared with disorderly-arranged ATP, the parallelly-arranged ATP shows a better gas diffusion channel and brings a more increase in gas permeability. Instead, the vertically-arranged ATP brings about a decrease in gas permeability. Additionally, introducing the ATP improves gas selectivity regardless of the arrangement of ATP. As long as gas permeates the narrow channels, they will be sieved and separated. As the content of ATP is 5 wt.%, the parallelly-arranged ATP/PIM-1 MMMs show CO_2 permeability of ~ 4000 Barrer coupled with good CO_2/N_2 selectivity of ~18 and O_2 permeability coefficient of ~670 Barrer coupled with good O_2/N_2 selectivity of ~3. It shows good potential to air separation.

ACKNOWLEDGEMENT

This work is supported by the National Natural Science Foundation of China (Grant No. 21978214). We would like to thank the Analytical & Testing Center of Tiangong University for providing technical support for SEM, TEM, and XRD et al.

CONFLICT OF INTEREST

The authors declare that they have no conflict of interest.

REFERENCES

1. Liang, L., Cai, Y., Gao, P., "A facile gas-driven ink spray (GDIS) deposition strategy toward hole-conductor-free carbon-based perovskite solar cells", *Emergent Mater.*, 5 (2022) 967-75.
2. Ebrahimi, P., Kumar, A., Khraisheh, M., "A review of recent advances in water-gas shift catalysis for hydrogen production", *Emergent Mater.*, 3 (2020) 881-917.
3. Monjezi, A. H., Mesbah, M., Rezakazemi, M., Younas, M., "Prediction bubble point pressure for CO_2/CH_4 gas mixtures in ionic liquids using intelligent approaches", *Emergent Mater.*, 4 (2021) 565-578.

4. De Guido, G.,"Cryogenic CO_2 capture from oxy-combustion flue gas by a hybrid distillation + physical absorption process", *Chem. Eng. Res. Des.*, 199 (2023) 639-658.
5. Aroon, M. A., Ismail, A. F., Matsuura, T., Montazer-Rahmati, M. M., "Performance studies of mixed matrix membranes for gas separation: A review", *Sep. Purif. Technol.*, 75 (2010) 229-242.
6. Matteucci, S., Yampolskii, Y., Freeman, Pinnau, I., "*Materials science of membranes for gas and vapor separation"*, Chichester: John Wiley & Sons, (2006).
7. Robeson, L. M., "The upper bound revisited", *J. Membr. Sci.*, 320 (2008) 390-400.
8. Robeson, L. M., "Correlation of separation factor versus permeability for polymeric membranes", *J. Membr. Sci.*, 62 (1991) 165-185.
9. Robeson, L. M., Smith, Z. P., Freeman, B. D., Paul, D. R., "Contributions of diffusion and solubility selectivity to the upper bound analysis for glassy gas separation membranes", *J. Membr. Sci.*, 453 (2014) 71-83.
10. Zhao, H. Y., Feng, L. Z., Ding, X. L., Zhao, Y., Tan, X. Y., Zhang, Y. Z., "The nitrogen-doped porous carbons/PIM mixed-matrix membranes for CO_2 separation", *J. Membr. Sci.*, 564 (2018) 800-805.
11. Zornoza, B., Esekhile, O., Koros, W. J., Téllez, C., Coronas J., "Hollow silicalite-1 sphere-polymer mixed matrix membranes for gas separation", *Sep. Purif. Technol.*, 77 (2011) 137-145.
12. Wijenay, ake, S. N., Panapitiya, N. P., Versteeg, S. H., Nguyen, C. N., Goel, S., Balkus, K. J., Musselman, I. H., Ferraris, J. P., "Surface cross-linking of ZIF-8/polyimide mixed matrix membranes (MMMs) for gas separation", *Ind. Eng. Chem.*, 52 (2013) 6991-7001.
13. Sen, M., Das, N., "In situ carbon deposition in polyetherimide/SAPO mixed matrix membrane for efficient CO_2/CH_4 separation", *J. Appl. Polym. Sci.*, 134 (2017) 45508.
14. Ridzuan, N. B., Musa, M. H., "Comparison between treated and untreated zeolite towards the performance of polyethersulfone mixed matrix membranes (MMMs) for O_2/N_2 gas separation", *Adv. Mat. Res.*, 550-553 (2012) 728-735.
15. Rezakazemi, M., Amooghin, A. E., Montazer-Rahmati, M. M., Ismail, A. F., Matsuura, T., "State-of-the-art membrane based CO_2 separation using mixed matrix membranes (MMMs): An overview on current status and future directions", *Prog. Polym. Sci.*, 39 (2014) 817-861.
16. Patel, N. P., Miller, A. C., Spontak, R. J., "Highly CO_2-permeable and selective polymer nanocomposite membranes", *Adv. Mater.*, 15 (2003) 729-733.
17. Hang, Y., Alkas, A., Zhang, Y. M., Zhang, Y. T., Telfer, S. G., "Mixed matrix membranes (MMMs) using an emerging metal-organic framework (MUF-15) for CO_2 separation", *J. Membr. Sci.*, 609 (2020) 118245.
18. Goh, P. S., Ng, B. C., Ismail, A. F., Sanip, S. M., Aziz, M., Kassim, M. A., "Effect of dispersed multi-walled carbon nanotubes on mixed matrix membrane for O_2/N_2 separation", *Sep. Sci. Technol.*, 46 (2011) 1250-1261.
19. Deng, J., Dai, Z. D., Deng, L. Y., "H_2-selective Troger's base-based mixed matrix membranes enhanced by 2D MOFs", *J. Membr. Sci.*, 610 (2020) 118262.
20. Chung, T. S., Lan, Y. J., Yi, L., Kulprathipanja, S., "Mixed matrix membranes (MMMs) comprising organic polymers with dispersed inorganic fillers for gas separation", *Prog. Polym. Sci.*, 32 (2007) 483-507.
21. Anson, M., Marchese, J., Garis, E., Ochoa, N., Pagliero, C., "ABS copolymer-activated carbon mixed matrix membranes for CO_2/CH_4 separation", *J. Membr. Sci.*, 243 (2004) 19-28.
22. Narwade V,. N., Bogle, K. A., Kokol V., "Hydrothermally synthesized hydroxyapatite cellulose composites thick films as ammonia gas sensor", *Emergent Mater.*, 5 (2022) 445-454.
23. Babaladimath, G., Rayar, A., Chapi, S., "Sugarcane bagasse valorized superabsorbent graft copolymer for efficient deposition of crystal violet and indigo carmine dyes from aqueous solutions", *Emergent Mater.*, 5 (2022) 1485–1493.
24. Haden, W. L., Schwint, I. A., "Attapulgite: Its proteries and applications", *Ind. Eng. Chem.*, 59 (1967) 58-69.
25. Suárez, M., García-Rivas, J., Morales, J., Lorenzo, A., García-Vicente, A., García-Romero, E., "Review and new data on the surface properties of palygorskite: A comparative study", *Appl. Clay Sci.*, 216 (2022) 106311.
26. Xiang, L., Pan, Y. C., Zeng, G. F., Jiang, J. L., Wang, C. Q., "Preparation of poly(ether-block-amide)/attapulgite mixed matrix membranes for CO_2/N_2 separation", *J. Membr. Sci.*, 500 (2016) 66-75.
27. Xiang, L., Pan, Y. C., Jiang, J. L., Chen, Y., Chen, J., Zhang, L. X., Wang, C. Q., "Thin poly(ether-block-amide)/attapulgite composite membranes with improved CO2 permeance and selectivity for CO_2/N_2 and CO_2/CH_4", *Chem. Eng. Sci.*, 160 (2017) 236-244.
28. Ahmad, S., Lian, S. H., Tan, Y. X., Li, R., Zhao, J., Song, C. F., Liu, Q. L., Lu, S. J., "Solvent influence on the textural properties and CO_2/N_2 separation performance of novel Pebax-1657/attapulgite mixed matrix membranes", *J. Environ. Chem. Eng.*, 9 (2021) 105806.

29. Wang, F., Zhang, B., Liu, S. S., Wu, Y. H., Wang, T. H., Qiu, J. S., "Investigation of the attapulgite hybrid carbon molecular sieving membranes for permanent gas separation", *Trans. Inst. Chem. Eng.*, 151 (2019) 146-156.
30. Zhao, H. Y., Xie, Q., Ding, X. L., Chen, J., Hua, M. M., Tan, X. Y., Zhang, Y. Z., "High performance post-modified polymers of intrinsic microporosity (PIM-1) membranes based on multivalent metal ions for gas separation", *J. Membr. Sci.*, 514 (2016) 305-312.
31. Schrader, B., "*Infrared and raman spectroscopy, methods and applications: Vibrational spectroscopy of different classes and states of compounds*", New York, VCH Publishers, (1995).
32. Melo, D., Ruiz, J., Melo, M., Sobrinho, E. V., Martinelli, A. E., "Compounds, preparation and characterization of lanthanum palygorskite clays as acid catalysts", *J. Alloys Compd.*, 344 (2002) 352-355.
33. Budd, P., Msayib, K. J., Tattershall, C. E., Ghanem, B. S., Reynolds, K. J, Mckeown, N. B., Fritsch, D., "Gas separation membranes from polymers of intrinsic microporosity", *J. Membr. Sci.*, 251 (2005) 263-269.
34. Wang, Z. G., Li, M. J., Zhang, X-F., Zhou, Y. C., Yao, J. F., "Integration of natural clay into cellulose membrane for efficient CO_2/N_2 separation", *Cellulose*, 29 (2022) 1873-1881.
35. Zhang, S. Y., Lu, X. C., Cai, M. W., Wang, Z., Han, Z. J., Chen, Z. Y., Liu, R. T., Li, K. X., Min, Y. G., "Attapulgite nanorod-incorporated polyimide membrane for enhanced gas separation performance", *Polymer*, 14 (2022) 5391.